Model of self assembled monolayer based molecular diodes made of ferrocenyl-alkanethiols

David Duche, Ujwol Planchoke, Florian-Xuan Dang, Judikaël Le Rouzo, Marc Bescond, Jean-Jacques Simon, Teodor Silviu Balaban, Ludovic Escoubas

▶ **To cite this version:**

David Duche, Ujwol Planchoke, Florian-Xuan Dang, Judikaël Le Rouzo, Marc Bescond, et al.. Model of self assembled monolayer based molecular diodes made of ferrocenyl-alkanethiols. Journal of Applied Physics, 2017, 121 (11), pp.115503. 10.1063/1.4978764 . hal-01683277

HAL Id: hal-01683277
https://hal.science/hal-01683277

Submitted on 16 Apr 2018

HAL is a multi-disciplinary open access archive for the deposit and dissemination of scientific research documents, whether they are published or not. The documents may come from teaching and research institutions in France or abroad, or from public or private research centers.

L'archive ouverte pluridisciplinaire **HAL**, est destinée au dépôt et à la diffusion de documents scientifiques de niveau recherche, publiés ou non, émanant des établissements d'enseignement et de recherche français ou étrangers, des laboratoires publics ou privés.

Model of self assembled monolayer based molecular diodes made of ferrocenyl-alkanethiols

David Duche,[1,a)] Ujwol Planchoke,[1] Florian-Xuan Dang,[2] Judikael Le Rouzo,[1] Marc Bescond,[1] Jean-Jacques Simon,[1] Teodor Silviu Balaban,[2] and Ludovic Escoubas[1]
[1]*Aix Marseille Universite, CNRS, Universite de Toulon, IM2NP UMR 7334, 13397 Marseille, France*
[2]*Aix-Marseille Universite, CNRS, Centrale Marseille, ISM2 UMR 7313, 13397, Marseille, France*

There has been significant work investigating the use of self assembled monolayers (SAMs) made of ferrocenyl terminated alkanethiols for realizing molecular diodes, leading to remarkably large forward-to-reverse current rectification ratios. In this study, we use a multiband barrier tunneling model to examine the electrical properties of SAM-based molecular diodes made of HSC_9Fc, $HSC_{11}Fc$, and HSC_iFcC_{13-i} $(0 \leq i \leq 13)$. Using our simple physical model, we reproduce the experimental data of charge transport across various ferrocenyl substituted alkanethiols performed by Nijhuis, Reus, and Whitesides [J. Am. Chem. Soc. **132**, 18386–184016 (2010)] and Yuan *et al.* [Nat. Commun. **6**, 6324 (2015)]. Especially, the model allows predicting the rectification direction in HSC_iFcC_{13-i} $(0 \leq i \leq 13)$ based molecular diodes depending on the position of the ferrocenyl (Fc) moiety within the molecules. We show that the asymmetry of the barrier length at both sides of the Highest Occupied Molecular Orbital of the ferrocenyl moiety strongly contributes to the rectifying properties of ferrocenyl-alkanethiol based molecular junctions. Furthermore, our results reveal that bound and quasi-bound states play an important role in the charge transport.

I. INTRODUCTION

In 1974, Aviram and Ratner[1] proposed the concept of a molecular diode. It is based on the idea that a molecule composed of a donor (D) group and an acceptor (A) group linked together by a σ bridge (a D-σ-A compound) would exhibit a natural rectification behavior. Since these first works, numerous researches related to molecular electronics have been carried out as this field promises the development of new nanoscale electronic components.[2–4] Molecular diodes functionalized with thiol linkers have strong advantages due to their ability to form self assembled monolayers (SAMs) covalently bound at the surface of noble metals (Ag and Au). It allows heterometallic nanogaps to be associated with organic molecules exhibiting diode behavior.[5] Furthermore, self-assembled molecular diodes can be coated at the surface of arrays of metallic nanostructures (nano-particles or nano-antennas) aiming at obtaining opto-electronic devices such as sensors,[6] selective filters,[7] or nano-rectennas.[8,9]

Molecular diodes made of ferrocenyl-containing alkanethiols are of great interest since they exhibit strong asymmetries, leading to remarkably large forward-to-reverse current rectification ratios (RR). The forward-to-reverse current rectification ratios (RR) can be used as a figure of merit to evaluate the rectifying properties of the molecular diodes. In our study, RR is defined as the ratio between the currents at -1 V and at 1 V

$$R = \frac{|J(-1V)|}{|J(1V)|}, \tag{1}$$

where $|J(\pm 1\,\mathrm{V})|$ is the absolute value of the current density (A/cm^2). Nijhuis, Reus, and Whitesides[10] and Yuan *et al.*[11] obtained RR greater than 100 using ferrocenyl-alkanethiol based molecular diodes in which both electrodes exhibited similar work functions. In this case, the rectification process was not governed by the work function difference between the electrodes but was due to the intrinsic rectifying properties of ferrocenyl-alkanethiols. Furthermore, Yuan *et al.*[11] experimentally showed very recently that a control of the direction of rectification is possible by placing the Fc units of ferrocenyl-alkanethiols (HSC_iFcC_{13-i}) at different positions within the alkyl chain.

In this study, we develop a multiband quantum transport model based on a matrix formulation[12] in which we consider both the HOMO (Highest Occupied Molecular Orbital) and LUMO (Lowest Unoccupied Molecular Orbital) levels and examine the electrical properties of the molecular junctions made of ferrocenyl-alkanethiols. The image potential in the potential barriers is also included in our model. We compare the computed current versus bias voltage I(Va) of the diodes under darkness with experimental measurements obtained by Nijhuis, Reus, and Whitesides,[10] and we give an insight into the physical phenomena occurring in ferrocenyl-alkanethiols based molecular diodes. Especially, we investigate through simulation how bound and quasi-bound states of the electronic levels of the molecules can participate in the charge transport. After this introduction, Section II of the paper is devoted to the description of the model developed to study the electrical properties of the molecular diodes. Section III is dedicated to the simulation of the electrical properties of HSC_9Fc and $HSC_{11}Fc$ based molecular diodes. We investigate

[a)]david.duche@im2np.fr

the influence of the HOMO and the LUMO energy bands of the ferrocene moiety and the alkyl chain length on the electrical properties of the diodes. In Section IV, we discuss the rectifying properties of HSC_iFcC_{13-i} ($0 \leq i \leq 13$) based molecular diodes depending on the position of the ferrocene (Fc) moiety within the molecules.

II. MODEL

In order to improve the understanding, we consider the specific case of a 11-(ferrocenyl)-1-undecane-thiol ($HSC_{11}Fc$) based molecular diode. As it is depicted in Figures 1(a) and 1(b), we consider a self-assembled monolayer (SAM) of $SC_{11}Fc$ sandwiched between two electrodes, forming a Metal-SAM-Metal diode. The first electrode is made of silver (Ag). The SAM is bound to the Ag electrode by covalent bounds between the sulfur and the Ag atoms (Ag-S). The second Ga_2O_3-EGaIn electrode is a eutectic liquid electrode usually used to fabricate molecular diodes. It is generally assumed that the terminated Fc moieties of the SAM form a Van der Walls contact with the Ga_2O_3-EGaIn electrode.[10,11] Figure 1(b) gives the theoretical band diagram (with respect to vacuum) of the resulting Ag-$SC_{11}Fc$-Ga_2O_3-EgGaIn molecular junction before the alignment of the Fermi levels. Both electrodes are defined by their work functions, allowing us to determine the Fermi level of the electrons in the metals. The alkyl chain of the molecule exhibits a large band gap with an HOMO well below the Fermi level of each electrode.[13] For this reason, the HOMO of the alkyl chain does not participate in the charge transportation and only the LUMO will be considered in the following. The ferrocenyl moieties are considered to be semiconductive, exhibiting HOMO and LUMO levels quite close to the Fermi level of each electrode. The exact position of the energy levels and their broadening will be discussed in detail in Section III.

We used a quantum transport model to examine the electrical properties of the molecular junctions. An electron is emitted from one of the two electrodes with a total energy E and is transferred through the potential barriers to the other electrode. The wave functions of the electron (Ψ) are given by the solutions of the time-independent Schrodinger equation. With the lack of an experimental estimate, the effective mass of the electron in the tunneling junction is assumed to be equal to the free electron mass (m_0).

A. Calculation of the barrier potential within the tunneling junction

The potential in the tunnel junction was considered to be invariant along both the transverse y and z axes. We assume

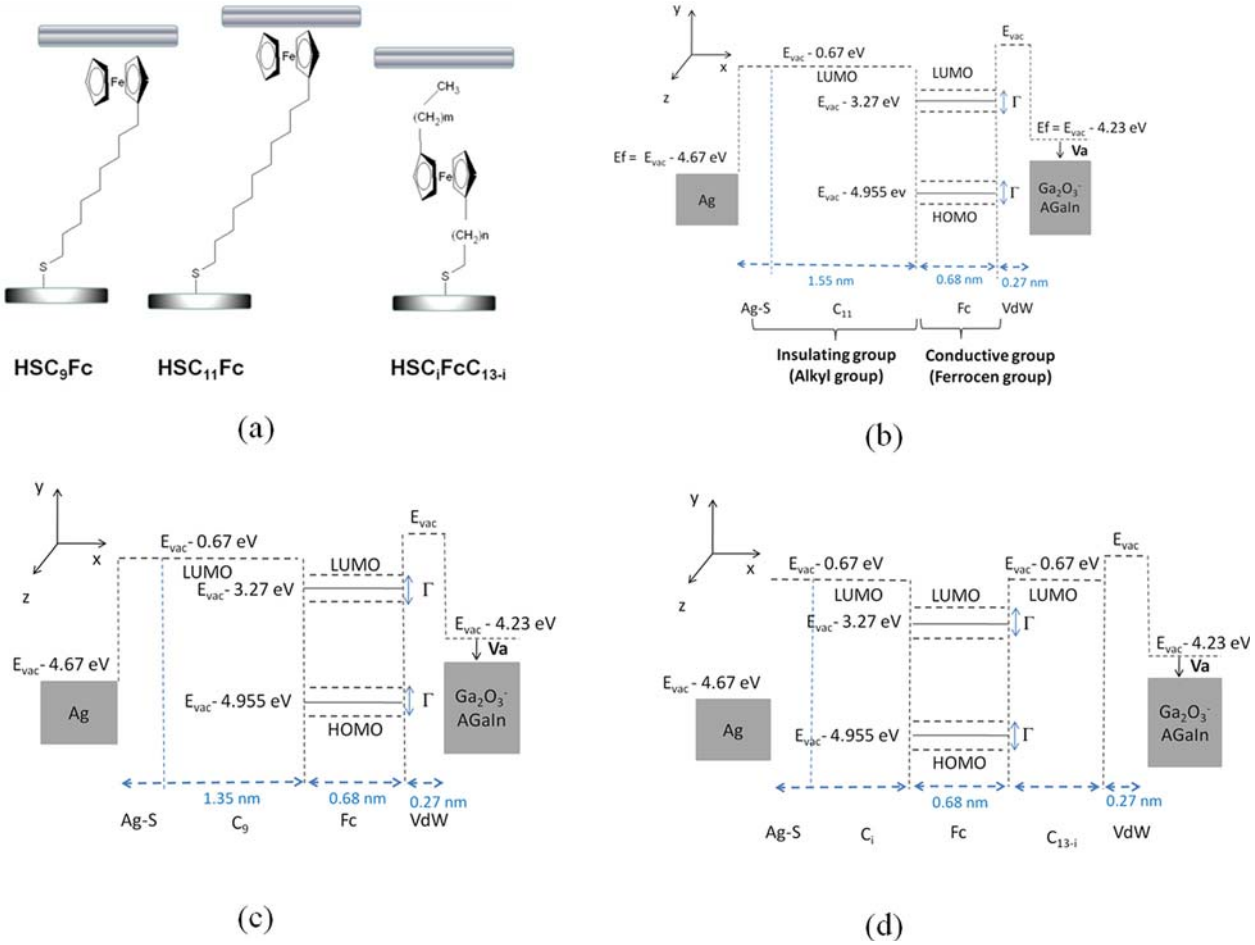

FIG. 1. (a) Schematic representation of molecular diodes made of ferrocenyl-containing alkanethiols. It consists of Ag bottom electrodes, SAM of SC_9Fc, $SC_{11}Fc$ or SC_iFcC_{13-I}, and Ga_2O_3-EGaIn electrodes. The theoretical energy band diagram of molecular diodes made of (b) $HSC_{11}Fc$, (c) HSC_9FC, and (d) HSC_iFcC_{13-i}.

the Fermi level of the left electrode to be 10 eV, but, as we will see in the following, the electrical properties of the diodes essentially depend on the energy relative to the vacuum level.[14] The potential variation (V (x)) within the junctions has been expressed as follows:

$$V(x) = W_L + \Delta\Phi + \frac{[(W_R - W_L) - qV_a]x}{d} + V_{image}, \quad (2)$$

where x is the distance of the electron from the left electrode, q is the elementary charge, d is the distance separating the two electrodes, and $W_L = W_{Ag}$ and $W_R = W_{Ga2O3-EgGaIn}$ are the work functions of the left silver electrode and the right Ga_2O_3–EgGaIn electrode, respectively. Va is the applied voltage (cf. Figure 1). The Va parameter is required in order to compute the I(Va) characteristics of the diodes and to examine their rectifying properties. In our model, we consider that a positive bias induces a decrease in the Fermi level of the right electrode and results in an additional potential within the junction. $\Delta\Phi$ is the energy difference between the work function of the left Ag electrode and the molecular orbital (HOMO or LUMO) of the functional groups located within the molecular junction. Within the Van der Waals' contacting, $\Delta\Phi$ is defined as the energy difference between the work function of the left electrode and the vacuum level. Because the relative dielectric constant of organic materials is low (~2), the image potential screening is weak within the molecular junctions.[15,16] Thus, an electron in the vicinity of an electrode "feels" an additional image potential, which results in barrier lowering. The solution of the image force problem results in an expression for the image potential $V_{image}(x)$, which is an infinite series[17]

$$V_{image}(x) = -\left(\frac{q^2}{4\pi\varepsilon_0\varepsilon_r}\right)\left[\frac{1}{2x} + \sum_{n=1}^{\infty}\frac{nd}{(nd)^2 - x^2} - \frac{1}{nd}\right], \quad (3)$$

where ε_0 and ε_r are the dielectric constant of the vacuum and the relative dielectric constant of the organic material within the junctions, respectively. The relative dielectric constant of the ferrocenyl-alkanethiols has been considered to be equal to the dielectric constant of the alkyl chains ($\varepsilon_r = 2.1$).[15] This expression can be accurately expressed by an hyperbolic function as follows:[17,18]

$$V_{image}(x) = -1.15.\frac{q^2\ln(2)}{8\pi\varepsilon_0\varepsilon_r d}.\frac{d^2}{x(d-x)}. \quad (4)$$

B. Calculation of the current density through the tunnel junction

Assuming an isotropic distribution of electron velocities in the metal electrodes, the tunneling current density through the junction can be calculated from the tunneling probability T[14,17,19]

$$I = \frac{4\pi m_0 q}{h^3}\int_{-\infty}^{\infty} T(E_x)dE_x \int_{E_x}^{\infty}\left[f_L(E) - f_R(E + qV_a)\right]dE, \quad (5)$$

where T is calculated using a matrix formalism.[12] The Fermi-Dirac distribution functions under bias in the left (f_L) and in the right (f_R) electrode are given by the following formula:[17]

$$f_L(E) = \frac{1}{1 + e^{\frac{E-E_{FL}}{KT}}}, \quad (6)$$

$$f_L(E) = \frac{1}{1 + e^{\frac{E-(E_{FL}-qV_a)}{KT}}}. \quad (7)$$

Due to the semi-conducting character of the ferrocenyl moiety, both the HOMO and the LUMO have to be considered. In our model, the contributions of the two levels are calculated separately. First, the tunneling current density J_{HOMO} is calculated by considering only the HOMO of the ferrocenyl moiety. In the same manner, the tunneling current density J_{LUMO} is calculated by considering only the LUMO of the ferrocenyl moiety. Finally, both tunneling current densities are added to obtain the total tunneling current density

$$J = J_{HOMO} + J_{LUMO}. \quad (8)$$

We have then implemented a ballistic transport model in which the energy E of an electron injected from the electrode remains constant along the active region of the system. Inelastic scattering phenomena, like interactions of electrons with phonons, are neglected. The simplicity of our physical model is an asset to give an insight into the physical phenomena occurring in molecular diodes. Furthermore, such a simple model does not require high computation resources and could be used for the optimization of the electrical properties of molecular diodes.[20]

III. $HSC_{11}Fc$ and HSC_9Fc based molecular diodes

We consider now an $HSC_{11}Fc$ based self-assembled molecular diode in the following configuration: Ag/SAM/Ga_2O_3-EGaIn. The shape of the potential barrier depends on the workfunctions of the electrodes, the HOMO and LUMO of the different functional groups within the ferrocenylalkanethiol, and the applied voltage. Figure 1(b) shows the energy band diagram of the diode. In accordance with the experimental work by Nijhuis, Reus and Whitesides,[10] we consider metallic Ag and Ga_2O_3-EGaIn electrodes with work functions of $W_{Ag} = 4.67$ eV and $W_{Ga2O3\text{-}EGaIn} = 4.23$ eV, respectively. The LUMO level of the alkyl chains is set to −0.67 eV. This value is in accordance with experimental measurements[21] and with values obtained through numerical simulations.[13,15] The energy position of the HOMO and the LUMO of the ferrocene moieties is −3.27 eV and −4.97 eV, respectively, while their broadenings (Γ) is varied between 0.1 eV and 0.7 eV. These values are in accordance with numerical simulations performed using the density functional theory (DFT) for an $HSC_{11}Fc$ based molecular diode in which both electrodes are made of gold (Au).[13] In the present work, starting from values extracted from Ref. 13, we adjust the energy position and the broadening of the HOMO and the LUMO to fit the data of the experimental work by Nijhuis, Reus and Whitesides.[10] This adjustment is necessary

because the electrical properties of the molecules are strongly influenced by the electrodes. Especially, the energy levels can be broadened within the molecular diode depending on the coupling strength between the electrons in the electrodes and those in the molecules.[11,22] The contacts at the Ag and the Ga_2O_3-EGaIn electrodes are totally different.[10] It is generally assumed that the Fc end group forms a Van der Waals contact with the Ga_2O_3-EGaIn[10] electrode, while the sulfur forms a covalent bond with the Ag electrode. As it can be seen in Figure 1, we consider an energy barrier equal to the one of the alkyl chain for the covalent bonds. For the Van der Waals contact, we consider a barrier potential corresponding to the vacuum level.

A. Influence of the Γ broadening

We first investigate the influence of the energy level broadening Γ on the electrical properties of $HSC_{11}Fc$ based diodes. The broadening of both the LUMO and the HOMO is varied independently. The other parameters are kept unchanged.

The HOMO level broadening (Γ_{HOMO}) is varied from 0.1 eV to 0.7 eV, while the LUMO level broadening is kept constant ($\Gamma_{LUMO} = 0.6$ eV). The resulting calculated I(Va) characteristics are presented in Figure 2(a). The HOMO level broadening mainly influences the diode electrical properties for negative applied voltages. A strong increase in the current is observed for applied voltages lower than −0.8 V when Γ_{HOMO} is higher than 0.57 eV. Thus, the I(Va) characteristics are highly asymmetric. This current increase is stable for broadenings varying between 0.57 eV and 0.7 eV. On the contrary, this current increase is becoming less and less pronounced when the broadening is decreasing from 0.57 eV to 0.1 eV, and the I(Va) characteristics become more and more symmetric. Figure 2(b) shows the I(Va) characteristics of the diode for different values of the LUMO level broadening ($0.1\,\text{eV} \leq \Gamma_{LUMO} \leq 0.7\,\text{eV}$). The LUMO level broadening mainly influences the slope of the I(Va) curves for positive applied voltages, but a smaller increase in the current can be observed. Thus, these calculations show that the rectification ratio is mainly influenced by the HOMO. In the following, we investigate the strong current increase occurring at negative applied voltages for the high values of the HOMO broadening. For these investigations, the LUMO broadening is fixed ($\Gamma_{LUMO} = 0.6$ eV), while two different values of the HOMO broadening have been considered ($\Gamma_{HOMO} = 0.6$ eV and $\Gamma_{HOMO} = 0.5$ eV).

Figure 3(a) shows the computed tunneling probability for $\Gamma_{HOMO} = 0.6$ eV ($\Gamma_{LU\ MO} = 0.6$ eV), and the computations are performed by considering only the HOMO of the ferrocenyl moiety. It allows computing the J_{HOMO} current density. The results are shown in color maps giving the tunneling probability as functions of both the electron energy (x-axis) and the applied voltage (y-axis). The black and gray lines give the energy positions of the Fermi levels of the left Ag electrode and the right Ga_2O_3−EGaIn electrode, respectively. Figure 3(a) reveals a sharp increase in the tunneling probability for energies ranging between 9.2 eV and 11 eV and for voltages ranging between 0 and −2 V. This region is surrounded by a dashed line in Figure 3(a). It corresponds to the presence of a resonant state in the HOMO of the ferrocenyl moiety. This resonance is shifted to higher energy values when the applied voltage is decreasing from 0 V to −2 V. It crosses the Fermi level of the left Ag electrode for Va = −1.06 V. When Va is decreasing from 0 V to −2 V, this resonance is approaching more and more the Fermi level of the left Ag electrode [the black line in Figure 3(a)]. Thus, the resonance participates more and more to the charge transportation. When the resonance is close enough to the Ag Fermi level (Va = −0.8 V), the current of the diode strongly increases [cf. Figure 2(a)]. The current continues to sharply increase until the resonance rises in the window between the Fermi levels of the two electrodes. This resonance corresponds to a bound state in the HOMO, which becomes a quasi-bound state when its energy position is higher than the Fermi level of the left electrode.[12] Figure 3(c) shows the transmission probability versus energy for an applied voltage of −1.06 eV. It clearly shows that a bound state, whose energy position corresponds to the Fermi level of the left Ag electrode (10 eV), exists. Figure 3(d) presents the potential inside the junction for $HSC_{11}Fc$ based diodes at Va = −1.06 V and for $\Gamma_{HOMO} = \Gamma_{LUMO} = 0.6$ eV. The dashed red line shows the energy position of the bound state within

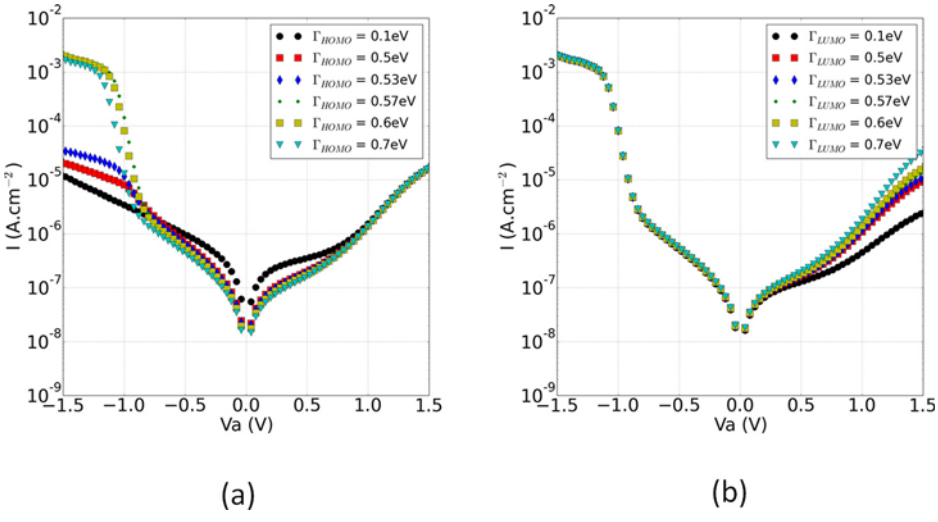

FIG. 2. Influence of the energy level broadening (a) Γ_{HOMO} and (b) Γ_{LUMO} on the calculated I(Va) characteristics of a $HSC_{11}Fc$ molecular diode.

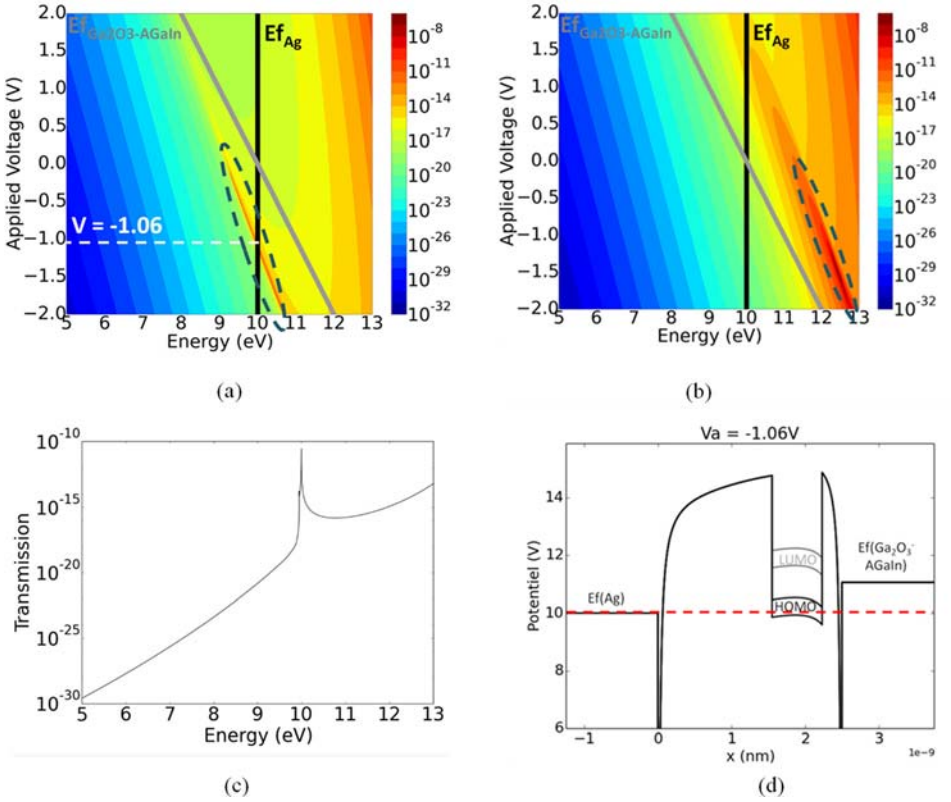

FIG. 3. (a) and (b) Computed color maps of the tunneling probability for the $HSC_{11}Fc$ based junction (by considering $\Gamma_{HOMO} = \Gamma_{LUMO} = 0.6\,eV$). The computations are performed considering (a) only the HOMO and (b) only the LUMO of the ferrocenyl moiety. The resonant states are surrounded by dashed lines. (c) and (d) The transmission probability versus energy for $Va = -1.06\,eV$ and the potential inside the $HSC_{11}Fc$ based molecular diode at $Va = -1.06\,V$ ($\Gamma_{HOMO} = \Gamma_{LUMO} = 0.6\,eV$), respectively.

the HOMO, which is equal to the Fermi level of the left electrode at $Va = -1.06\,eV$. Figure 3(b) shows the calculated tunneling probability map by considering only the LUMO of the ferrocenyl moiety ($\Gamma_{LUMO} = 0.6\,eV$) and allows to compute the current density J_{LUMO}. It reveals the presence of a quasi-bound state (red line) at high energy (12 to 13 eV) and for negative applied voltage (0 to $-2\,V$). Because this resonance never falls within the window between the Fermi levels of both electrodes, it does not strongly participate in the charge transportation.

Figure 4(a) shows the calculated tunneling probability for $\Gamma_{HOMO} = 0.5\,eV$. As previously reported, these computations are performed by only considering the HOMO of the ferrocenyl moiety. In contrast to the previous results,

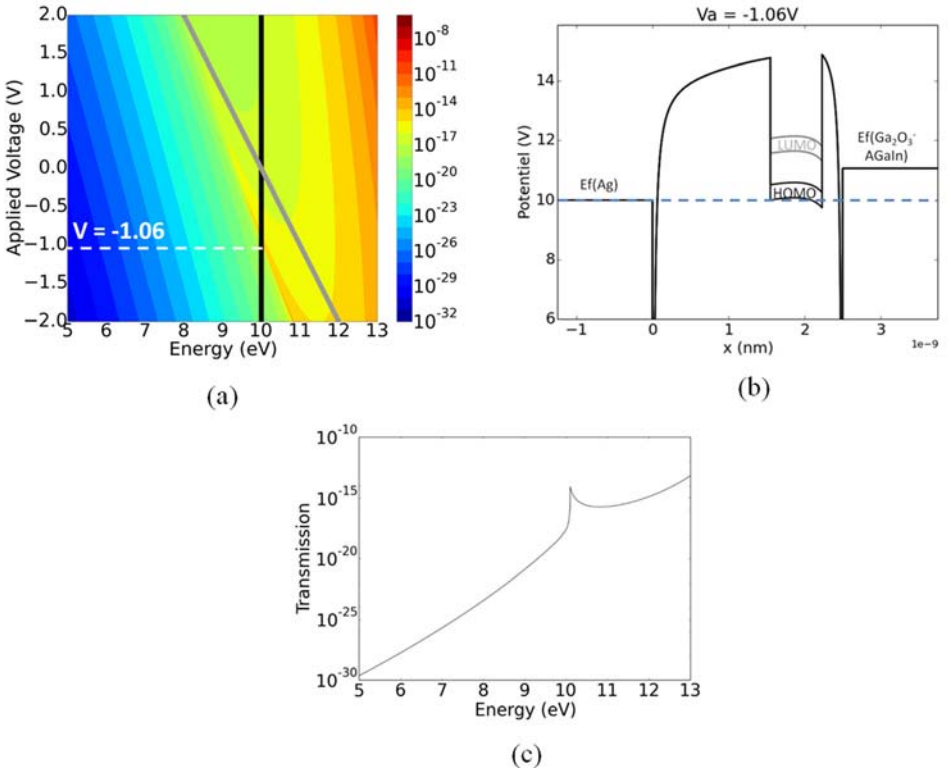

FIG. 4. (a) Computed color map of the tunneling probability for the $HSC_{11}FC$ based junction by considering $\Gamma_{HOMO} = \Gamma_{LUMO} = 0.5\,eV$. The computations are performed considering only the HOMO of the ferrocene moiety. (b) and (c) The transmission probability versus energy for $Va = -1.06\,eV$ and the potential inside the $HSC_{11}Fc$ based molecular diode at $Va = -1.06\,V$ ($\Gamma_{HOMO} = \Gamma_{LUMO} = 0.5\,eV$), respectively.

Figure 4(a) does not reveal a sharp increase in the tunneling probability for energies ranging between 9.2 eV and 11 eV and for voltages ranging between 0 and −2 V. Thus, the resonant state coupling within the HOMO previously observed for $\Gamma_{HOMO} = 0.6$ eV is less pronounced for $\Gamma_{HOMO} = 0.5$ eV. Figure 4(c) shows the transmission probability versus energy for an applied voltage of −1.06 eV. The transmission probability at 10 eV is less sharp than previously reported. We explain these results by the fact that the resonant state cannot be coupled efficiently within the HOMO. Figure 4(b) gives the potential inside the $HSC_{11}Fc$ based junction at Va = −1.06 V and for $\Gamma_{HOMO} = 0.5$ eV and $\Gamma_{LUMO} = 0.6$ eV. The blue dashed line is located at the Fermi level of the left electrode, which corresponds to the energy level at which the bound state should be coupled. These results reveal that the bound state is not located within the HOMO. Figure 4(b) shows that the HOMO is located between the Fermi level of both electrodes at Va = −1.06 V. Thus, because the HOMO rises between the Fermi levels of both electrodes, we can observe a slight increase in the current for applied voltages lower than −0.8 V (cf. Figure 2(a)). Nevertheless, our results reveal that the HOMO is not large enough to allow a bound state appearing. It may explain why the asymmetry of the I(Va) characteristics is weakly pronounced for $\Gamma_{HOMO} = 0.5$ eV (cf. Figure 2(a)).

These results are in accordance with the mechanism proposed by Nijhuis, Reus, and Whitesides[10] and by Cui *et al.*[13] for the current rectification by $HSC_{11}Fc$ SAM based molecular junctions. They suggested that the large rectification observed for $HC_{11}Fc$ molecular junctions originates from the accessible HOMO of the Fc moiety, which is asymmetrically positioned in the junction and electronically coupled to one electrode through non-uniform potential drops. According to recent theoretical works,[16] our computations show that the molecular orbital width Γ_{HOMO} is an important parameter influencing the rectification ratio of the diodes. Furthermore, our results reveal that bound or quasi-bound states may play a crucial role in the charge transportation within $HSC_{11}Fc$ based molecular junctions.

B. Influence of the energy position

We investigate the influence of the energy position of the HOMO and LUMO on the electrical properties of $HSC_{11}Fc$ based diodes. For this purpose, the broadening of both the HOMO and LUMO levels is fixed ($\Gamma_{HOMO} = \Gamma_{LUMO} = 0.6$ eV). The energy position of the HOMO is first varied between −4.64 eV and −5.17 eV, while the energy position of the LUMO is kept constant at −3.27 eV. Figure 5(a) shows that the strong current increase in the junction is shifted to lower negative applied voltages (Va) when the energy position of the HOMO decreases. In other words, when the energy position of the HOMO decreases, a stronger negative applied voltage is required to raise the HOMO between the Fermi levels of both electrodes. Then, the energy position of the LUMO is varied between −3.47 eV and −3.07 eV, while the energy position of the HOMO is kept at −4.97 eV. The results are shown in Figure 5(b) and reveal that the energy position of the LUMO mainly influences the slope of the I(Va) curve at positive bias. Thus, the closer is the LUMO to the Fermi level of the right electrode, the lower is the resistivity of the junction at positive bias. These results show that the HOMO electrode work function offset strongly influences the diode rectification ratios.

C. Influence of the alkyl chain length

Finally, the energy level positions and the level broadenings are adjusted to fit the experimental I(Va) characteristics obtained by Nijhuis, Reus, and Whitesides.[10] For the HOMO, the obtained energy position and broadening are −4.955 eV and 0.57 eV, respectively. For the LUMO, the obtained energy position and broadening are −3.27 eV and 0.57 eV, respectively. The distance between the end of the molecule and the right electrode is adjusted at 0.27 nm. Figure 6(a) shows that the computed I(Va) characteristic of the $HSC_{11}Fc$ based junction agrees quite well with experimental measurements. The difference between the experimental and the computed data may be due to the fact that, for the computations, we consider perfect monolayers as depicted in Figure 1(a), while the experimental data published by Nijhuis, Reus, and Whitesides[10] have been averaged on large numbers of data (N = 300–1000). The calculated RR (from Equation (1)) between Va = −1 V and Va = 1 V is 109, while Nijhuis, Reus, and Whitesides experimentally obtained a RR of 100.[10] Figure 6(b) depicts the

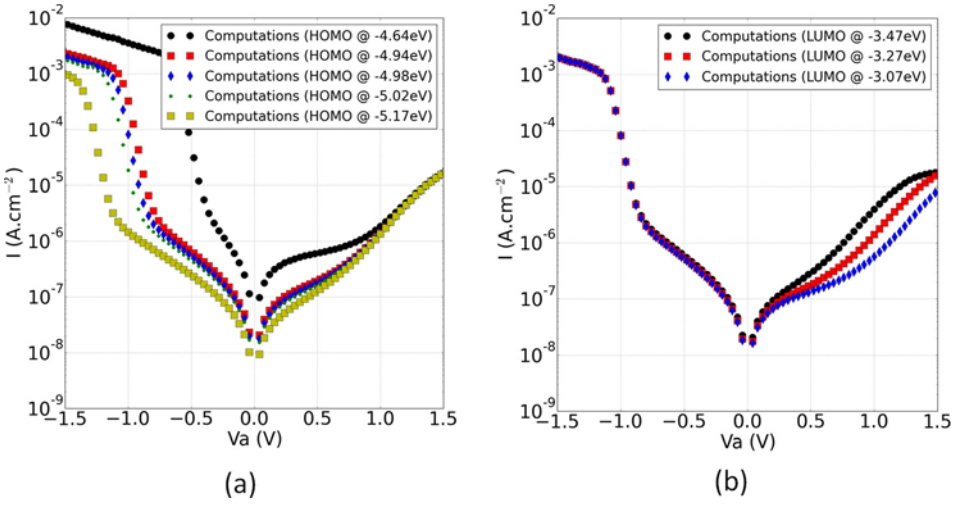

FIG. 5. Influence of the (a) HOMO and (b) LUMO energy positions on the I(Va) characteristic of the $HSC_{11}Fc$ based molecular junction.

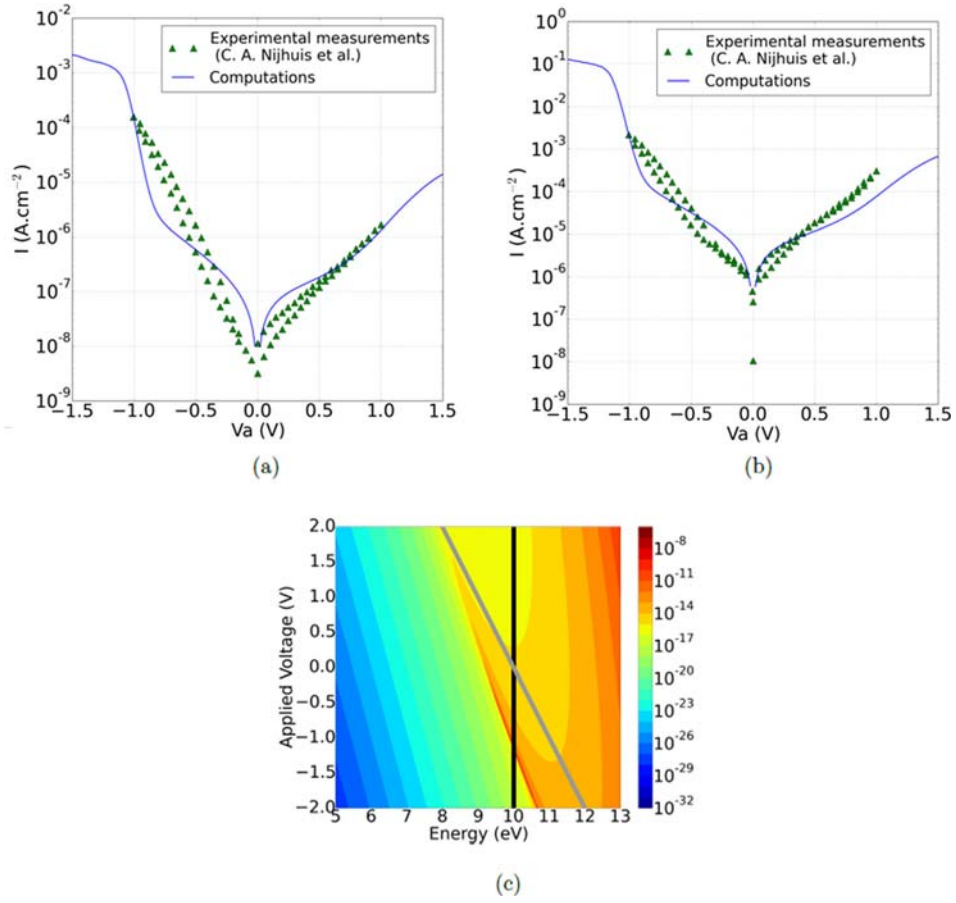

FIG. 6. Comparison between computed I(Va) characteristics and experimental measurement obtained by Nijhuis, Reus, and Whitesides[10] for (a) a $HSC_{11}Fc$ based molecular junction and (b) a HSC_9Fc based molecular junction. (c) A color map of the tunneling probability for the HSC_9FC based molecular diode ($\Gamma_{HOMO} = 0.57$ eV and $\Gamma_{LUMO} = 0.6$ eV).

computed I(Va) characteristic of HSC_9FC based molecular diodes. As shown in Figures 1(b) and 1(c), while the whole length of HSC_{11} including the covalent bond (S-Ag) is 1.55 nm, the length of HSC_9 is reduced to 1.35 nm.[10] The other parameters are identical to those used for the $HSC_{11}Fc$ based molecular diode. The computed I(Va) curve reproduces quite well the experimental data of the work by Nijhuis, Reus, and Whiteside[10] and reveals a strong increase in the current at reverse bias. The calculated RR between $Va = -1$ V and $Va = 1$ V is 26, while Nijhuis, Reus, and Whitesides experimentally obtained a RR of 10.[10] Figure 6(c) shows the color map of the tunneling probability computed for the HSC_9Fc based diode and performed by only considering the HOMO of the ferrocenyl moiety. This figure reveals a resonant state for energies ranging between 9.2 eV and 11 eV and for voltages ranging between 0 and −2 V. While this resonance is crossing the Fermi level of the left Ag electrode at $Va = -1.06$ eV in the case of $HSC_{11}Fc$, it now crosses the Fermi level of the left Ag electrode at $Va = -1.13$ V. Thus, the resonant state rises between the Fermi levels of both electrodes at lower negative voltages, and the calculated rectification ratio of the HSC_9Fc based diode is lower than the one of the $HSC_{11}Fc$ diode.

IV. INFLUENCE OF THE FERROCENYL POSITION WITHIN THE MOLECULAR JUNCTION

In this section, we investigate the influence of the ferrocenyl position within the molecular junction on the rectifying properties of the molecular diodes. Figure 1(d) gives the theoretical band diagram of HSC_iFcC_{13-i} based molecular diodes having Ag and Ga_2O_3−EgGaIn electrodes. Both the CH_3 and Fc end groups form Van der Waals interactions with the Ga_2O_3−EgGaIn electrode, and the sulfur forms a covalent bounding with the Ag electrode. Our model does not take into account the fact that the broadening of the HOMO level may increase exponentially when the Fc moiety is very close to the Ag electrode.[16] Nevertheless, as it will be presented in the following, this model is able to reproduce the main electrical behavior of the HSC_iFcC_{13-i} based molecular diodes, which tends to prove that the asymmetry of barrier lengths at both sides of the HOMO also strongly contributes to the rectifying properties of the junctions.

As previously reported, the HOMO energy position and broadening are fixed at −4.955 eV and 0.57 eV, respectively. These values are in strong accordance with the values obtained from experimental UPS measurements. Indeed, a HOMO energy position around −5 eV and a HOMO broadening between 0.5 eV and 0.75 eV have been obtained from UPS measurements.[11,16] Figures 7(a) and 7(d) show the computed I(Va) characteristics of $HSC_{13}Fc$ and $HSFcC_{13}$ based molecular junctions, respectively. In accordance with the experimental measurements obtained by Nijhuis *et al.*,[11] while the $HSFcC_{13}$ based diode rectifies the current at forward bias, the $HSC_{13}Fc$ based diode rectifies the current at opposite bias. Figures 7(b) and 7(e) show the color map of the tunneling probability computed for the $HSC_{13}Fc$ and $HSFcC_{13}$ based diodes, respectively. These computations are performed by considering only the HOMO of the ferrocenyl moiety. As previously reported, Figure 7(b) reveals bound

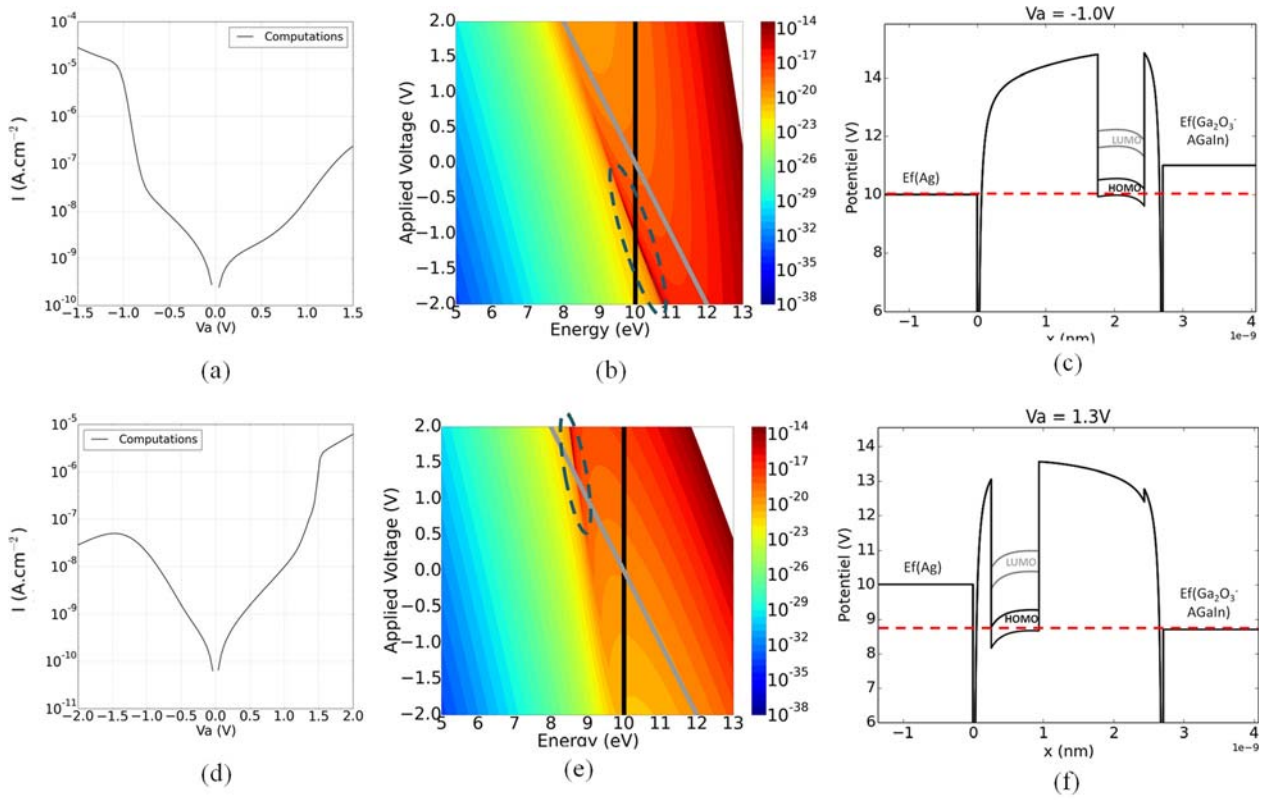

FIG. 7. Computed (a) I(Va) characteristics, (b) color map of the tunneling probability, and (c) potential inside the molecular junction for a $HSC_{13}Fc$ based diode. Computed (d) I(Va) characteristics, (e) color map of the tunneling probability, and (f) potential inside the molecular junction for a $HSFcC_{13}$ based diode.

and quasi-bound states within the HOMO of the Fc moiety for negative bias. This resonant state crosses the Fermi level of the left Ag electrode at $Va = -1.0\,V$ and is responsible for the strong increase in the current at negative bias. Figure7(c) gives the potential inside the junction at $Va = -1.0\,V$. The red dashed line is located at the Fermi energy level of the left Ag electrode which is equal to the energy position of the resonant state at $Va = -1.0\,eV$. Figure 7(e) gives the color map of the tunneling probability of the $HSFcC_{13}$ based junction. In this case, we observe bound and quasi-bound states at positive bias. This resonant state crosses the Fermi level of the right Ga_2O_3–EgGaIn electrode at $Va = 1.3\,V$ and is responsible of the strong increase in the current at positive bias. When Va increases from 0 V, the HOMO enters the window between both electrodes and the resonant state is approaching more and more the Fermi level of the right Ga_2O_3–EgGaIn electrode. When the resonance is close enough to the Ga_2O_3–EgGaIn Fermi level, the diode current strongly increases. The current continues to sharply increase until the resonance falls into the window between the Fermi levels of the two electrodes. Figure 7(f) gives the potential inside the junction at $Va = 1.3\,V$. The red dashed line is located at the Fermi energy level of the right Ga_2O_3–EgGaIn electrode which is equal to the energy position of the resonant state at $Va = 1.3\,V$.

Figure 8(a) shows the computed I(Va) characteristic of a HSC_6FcC_7 based diode ($\Gamma_{LUMO} = \Gamma_{HOMO} = 0.53\,eV$). In this configuration, the Fc moiety is separated from both

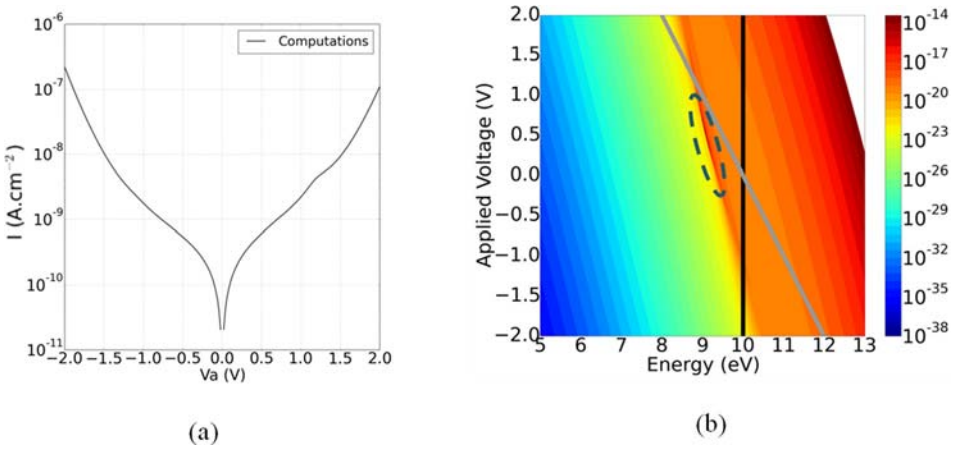

FIG. 8. Computed (a) I(Va) characteristics and (b) color map of the tunneling probability of a HSC_6FcC_7 based diode.

electrodes by an alkyl chain (cf. 1(d)). In accordance with the experimental results obtained by Nijhuis *et al.*,[11] the I(Va) characteristic is highly symmetric and the diode exhibits a rectification ratio close to unity (no rectification). Figure 8(b) shows the color map of the tunneling probability through the junction by considering only the HOMO of the ferrocenyl moiety. Figure 8(b) reveals a bound state within the HOMO of the Fc moiety for negative and positive bias. This resonant state does not cross any electrode Fermi level in the considered range of applied voltages. Thus, they do not participate actively in the charge transportation either at positive voltages or at negative voltages, which nicely explains why the I(Va) curve is symmetric. In other words, the accessible HOMO of the Fc moiety is symmetrically positioned in the junction, which results in a symmetric electronic coupling to both electrodes. The potential drop within the junction is too low to ensure that the bound state enters the window between the Fermi levels of the electrodes.

V. CONCLUSION

We have developed a simple but efficient and reliable 1D multiband quantum transport model considering both the HOMO and LUMO levels to investigate the electrical properties of molecular diodes made of ferrocenyl-alkanethiols. Our results suggest that the large rectification ratio observed for HC11Fc molecular junctions originates from the accessible HOMO of the Fc moiety which is asymmetrically positioned in the junction and electronically coupled to one electrode through non-uniform potential drops. Our results reveal that bound or quasi-bound states play an important role in the charge transportation in the molecular diodes. The computed I(Va) characteristics of $HSC_{11}Fc$ and HSC_9FC based junctions agree well with experimental measurements obtained by Nijhuis, Reus, and Whitesides.[10] The calculated RR between $Va = -1\,V$ and $Va = 1\,V$ is 109 and 26 for $HSC_{11}Fc$ and HSC_9FC based junctions, respectively, while Whiteside *et al*. experimentally obtained RR of 100 and 10 for $HSC_{11}Fc$ and HSC_9FC based junctions, respectively.[10] We show that our model allows explaining and predicting the electrical properties of molecular diodes made of HSC_iFcC_{13-i}. In accordance with the experimental results obtained by Yuan *et al.*,[11] we show that the direction of rectification depends on the position of the Fc units within the alkyl chain of ferrocenyl-alkanethiol. Finally, our model allows extracting electronic properties of the ferrocenylalkanethiol such as the orbital energy positions and the orbital widths. Furthermore, this model has the advantage that it does not require DFT or TD-DFT time consuming computations.

ACKNOWLEDGMENTS

This work was carried out thanks to the support of the A*MIDEX project (No. ANR-11-IDEX-0001-02) funded by the "Investissements d'Avenir" French Government program and managed by the French National Research Agency (ANR).

[1]A. Aviram and M. A. Ratner, Chem. Phys. Lett. **29**, 277 (1974).
[2]G. Ashwell and A. Mohib, J. Am. Chem. Soc. **127**(46), 16238 (2005).
[3]E. Lörtscher, V. Geskin, B. Gotsmann, J. Fock, J. Sorensen, T. Bjornholm, J. Cornil, H. van der Zant, and H. Riel, Small **9**(2), 209 (2013).
[4]H. Vazquez, R. Skouta, S. Schneebeli, M. Kamenetska, R. Breslow, L. Venkataraman, and M. Hybertsen, Nat. Nanotechnol. **7**(10), 663 (2012).
[5]X. Chen, S. Yeganeh, L. Qin, S. Li, C. Xue, A. Braunschweig, G. Schatz, M. Ratner, and C. Mirkin, Nano Lett. **9**(12), 3974 (2009).
[6]A. D. McFarland and R. P. V. Duyne, Nano Lett. **3**, 1057 (2003).
[7]J. C. Love, L. A. Estroff, J. K. Kriebel, R. G. Nuzzo, and G. M. Whitesides, Chem. Rev. **105**, 1103 (2005).
[8]D. Goswami, S. Vijayaraghavan, S. Lu, and G. Tamm, Sol. Energy **76**, 33 (2004).
[9]J. M. Nunzi, Proc. SPIE **7712**, 771204 (2010).
[10]C. A. Nijhuis, W. F. Reus, and G. M. Whitesides, J. Am. Chem. Soc. **132**, 18386 (2010).
[11]L. Yuan, N. Nerngchamnong, L. Cao, H. Hamoudi, E. del Barco, M. Roemer, R. K. Sriramula, D. Thompson, and C. A. Nijhuis, Nat. Commun. **6**, 6324 (2015).
[12]A. K. Ghatak, K. Thyagarajan, and M. R. Shenoy, IEEE J. Quantum Electron. **24**(8), 1524 (1988).
[13]B. Cui, Y. Xu, G. Ji, H. Wang, W. Zhao, Y. Zhai, D. Li, and D. Liu, Org. Electron. **15**, 484 (2014).
[14]S. Grover and G. Moddel, Solid-State Electron. **67**, 94 (2012).
[15]H. B. Akkerman, R. C. G. Naber, B. Jongbloed, P. A. van Hal, P. W. M. Blom, D. M. de Leeuw, and B. de Boer, Proc. Natl. Acad. Sci. U.S.A. **104**, 11161 (2007).
[16]A. R. Garrigues, L. Yuan, L. Wang, E. R. Mucciolo, D. Thompon, E. del Barco, and C. A. Nijhuis, Sci. Rep. **6**, 26517 (2016).
[17]J. G. Simmons, J. Appl. Phys. **34**(6), 1793 (1963).
[18]O. M. Probst, Am. J. Phys. **70**(11), 1110 (2002).
[19]J. G. Simmons, J. Phys. D: Appl. Phys. **4**(5), 613 (1971).
[20]N. Armstrong, R. C. Hoft, A. McDonagh, M. B. Cortie, and M. J. Ford, Nano Lett. **7**(10), 3018 (2007).
[21]A. Salomon, D. Cahen, S. Lindsay, J. Tomfohr, V. B. Engelkes, and C. D. Frisbie, Adv. Mater. **15**, 1881 (2003).
[22]K. Moth-Poulsen and T. bjornholm, Nat. Nanotechnol. **4**, 551 (2009).